pubs.acs.org/Biomac

Article

Aldehyde-Assisted Lignocellulose Fractionation Provides Unique Lignin Oligomers for the Design of Tunable Polyurethane Bioresins

Richard Vendamme,* Jean Behaghel de Bueren, Jaime Gracia-Vitoria, Florence Isnard, Mikael Monga Mulunda, Pablo Ortiz, Mohan Wadekar, Karolien Vanbroekhoven, Chloé Wegmann, Raymond Buser, Florent Héroguel, Jeremy S. Luterbacher, and Walter Eevers

Cite This: *Biomacromolecules* 2020, 21, 4135–4148

Read Online

ACCESS | Metrics & More | Article Recommendations | Supporting Information

ABSTRACT: Thanks to chemical stabilization, aldehyde-assisted fractionation (AAF) of lignocellulosic biomass has recently emerged as a powerful tool for the production of largely uncondensed lignin. Depolymerization of AAF lignin via ether cleavage provides aromatic monomers at near theoretical yields based on ether cleavage and an oligomeric fraction that remains largely unexploited despite its unique material properties. Here, we present an in-depth analytical characterization of AAF oligomers derived from hardwood and softwood in order to elucidate their molecular structures. These bioaromatic oligomers surpass technical Kraft lignin in terms of purity, solubility, and functionality and thus cannot even be compared to this common feedstock directly for material production. Instead, we performed comparative experiments with Kraft oligomers of similar molecular weight (Mn ∼ 1000) obtained through solvent extraction. These oligomers were then formulated into polyurethane materials. Substantial differences in material properties were observed depending on the amount of lignin, the botanical origin, and the biorefining process (AAF vs Kraft), suggesting new design principles for lignin-derived biopolymers with tailored properties. These results highlight the surprising versatility of AAF oligomers towards the design of new biomaterials and further demonstrate that AAF can enable the conversion of all biomass fractions into value-added products.

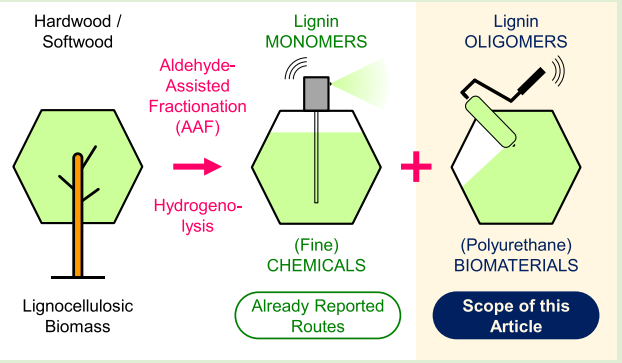

INTRODUCTION

Global climate change and the depletion of finite feedstocks are strong drivers for the chemical and polymer industries to develop more sustainable processes based notably on the renewability of their energy sources and feedstocks.[1,2] In this context, in 2019, the World Economic Forum (WEF) listed the development of bioplastics as one of the top 10 emerging technologies expected to widely impact the global social and economic order.[3] The WEF specifically emphasized that the valorization of lignin towards bioplastics is of particular relevance because the structure of lignin is composed of (bio) aromatic rings, the chemical structures that provide mechanical strength, rigidity, and other desirable features to many common plastics and resins.[4]

Lignin is the second most abundant natural polymer and the largest natural source of aromatic monomers. It represents an enormous, but yet underutilized, source of renewable carbon with the potential to serve as a feedstock for fuels, chemicals, and materials.[5,6] Today, lignin is mostly produced as an industrial residue of pulp and paper factories (for instance, as a byproduct of the Kraft process), and most of the several million tons of lignin produced annually are utilized as a low-cost fuel for power and heat generation.[7,8] This highlights the need for new strategies for valorizing lignin as an abundant macromolecular building block for the design of more sustainable and functional bioplastics.

Polyurethanes are synthesized from the reaction between polyols and isocyanates (NCO) and represent an extremely diverse set of polymeric materials exhibiting a wide range of properties suitable for various applications and market segments such as foams, elastomers, coatings, adhesives, or fibers. The versatility of polyurethane chemistry originates from the possibility to control the properties of the final materials by tuning the chemical structure and the branching/cross-linking of their polymer constituents.[9] Globally, polyurethanes had a market size of $ 60.5 billion in 2017, roughly corresponding to 16.9 million tons of products, and have seen continuous growth in recent years. The growing attention towards sustainable development is pushing the polyurethane

Received: June 17, 2020
Revised: August 20, 2020
Published: August 26, 2020

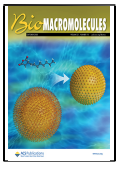

https://dx.doi.org/10.1021/acs.biomac.0c00927
Biomacromolecules 2020, 21, 4135–4148

(PU) industry to integrate more renewable content and lower the carbon footprint of its products. To this end, renewable polyols provide attractive avenues for designing more sustainable and partially biobased PU materials. Typical examples include green polyols derived from vegetable oils or from sugars.[10,11]

In this context, lignin has long been considered a renewable aromatic macropolyol that could potentially replace conventional fossil-derived polyols in PU synthesis because of its high concentration of hydroxyl groups (both aliphatic and phenolic) that could react with isocyanates to achieve PU linkages. However, despite the long history of lignin PU synthesis, several issues are still preventing the more widespread integration of lignin in PU products.[12] The synthetic challenges for designing lignin PU are well known[13] and are generally attributed to (1) the low solubility of lignin (in solvents or with the other PU precursors), resulting in its poor incorporation into the polymer matrix, in low reactivity with the co-reactants, and the impossibility to use common organic solvents, (2) the high molecular weight of lignin, which creates steric hindrances, further limiting its reactivity, (3) its high polydispersity, which leads to inconsistent performance, reactivities, and solubilities, (4) its sulfur content that can generate odor problems and yellowing of final products, and (5) lignin's dark color that prevents its use in certain applications including coatings. Most of the efforts reported so far have focused on the design of lignin PU systems derived from widely available technical lignin such as unfractionated Kraft lignin. Therefore, the challenges mentioned above could also largely be associated with the use of such feedstock.

One strategy for trying to overcome these limitations is to chemically modify technical lignins (e.g., via oxypropylation, esterification, or etherification).[14−16] However, although this approach has the benefit to increase the reactivity of the OH groups and improve the compatibility, the chemical modifications increase the cost of the process and do not resolve other issues, which include high lignin polydispersity. An increasingly popular approach to overcome the above-mentioned challenges relies on the separation of purified fractions of lignin with lower molecular weight and narrower polydisperisty obtained via solvent extraction or membrane filtration.[17−21] For instance, solvent-extracted softwood Kraft lignin has recently been employed as a base polymer for the design of thermosetting epoxy resins[22] and polyurethane materials[23,24] or tough self-healing elastomers.[25] The major drawback of this approach is that only the (small) soluble fraction of lignin is being valorized, while the rest is mostly wasted and do not contribute to the overall economic valorization of the biorefining process.

Besides these approaches based on technical lignin, several lignin valorization strategies have emerged in which the lignin is first depolymerized to smaller, more reactive and more miscible bioaromatic compounds before being valorized in higher added-value applications.[26,27] A major challenge with these depolymerization strategies is the necessity to limit the formation of recalcitrant interunit carbon−carbon bonds, preventing efficient lignin deconstruction.[28] Thanks to an efficient stabilization strategy, aldehyde-assisted fractionation (AAF) of lignocellulosic biomass has recently emerged as a powerful tool for the production of uncondensed lignin.[29] Depolymerization of AAF lignin provides aromatic monomers at near-theoretical yields and an oligomeric fraction, which remain unexplored to date despite its unique material properties.[30]

Here, we present an in-depth analytical characterization of AAF oligomers derived from hardwood and softwood in order to elucidate their molecular structures, before designing AAF oligomer-based PU systems. Because these bioaromatic oligomers surpass technical lignin in terms of solubility, purity, and functionality, we performed comparative experiments with more soluble pre-extracted Kraft oligomers of comparable molecular weight (Mn ∼ 1000) using methyl ethyl ketone (MEK) as the extraction solvent. These oligomers were then formulated into polyurethane materials in order to elucidate the structure−property relationships of the materials and highlight the unique features of the AAF oligomers as compared to the pre-extracted oligomers.

EXPERIMENTAL SECTION

Materials and Chemicals. *Lignin Oligomers.* For the preparation of the AAF oligomers, softwood (mixture of spruce and pine) chips were provided by Patrick Arnold (Switzerland) and hardwood (beech) chips were provided by Michael Studer (Switzerland). For the complete procedure of the preparation of the AAF oligomers, the reader is kindly asked to refer to the Supporting Information. Softwood (pine) Kraft lignin was purchased from the LignoBoost demonstration plant of RISE (Sweden). Hardwood (eucalyptus) Kraft lignin was obtained from Fribia (Brazil). Protocol for the pre-extraction of Kraft lignin oligomers can be found in the Supporting Information.

Polyurethane Precursors. Hexamethylene diisocyanate trimer Desmodur ultra N 3600 was purchased from Covestro. Polytetrahydrofuran (PTHF, Mw = 650 g/mol), tin octanoate, dry MEK, and the solvents considered in this work were purchased from Alfa Aesar or Sigma-Aldrich and were used as received.

Synthesis of Lignin PU Films. *Protocol.* In a vial, the catalyst (tin octanoate, 0.8 mol %), the desired lignin, and copolyol (PTHF) were dissolved in dry MEK (8 mL for 2 g of total formulation) and stirred at RT until complete dissolution. Afterward, isocyanate was added to the solution, and the temperature was increased to 40 °C. The reaction was carried out for 1 h. The solution was poured into Teflon molds (70 × 35 × 2 mm), the solvent was evaporated slowly overnight at RT, and curing was further performed in the oven for 6 h at 100 °C. The films were stored for at least 1 week before any characterization.

Effect of the NCO/OH Ratio on PU Properties. In this work, the NCO/OH ratio was fixed at 0.9. Lignin PU with higher NCO/OH ratios (1.1 or 1.3) have also been synthesized with AH oligomers but are not reported in this article. A slight excess of NCO groups automatically decrease the lignin weight ratio in the material but could represent an advantage for designing a tougher material. For instance, AH100PU (r = 0.9) is a quite brittle rigid network, while AH100PU/1.3 (r = 1.3) is still rigid but less brittle. In general, higher NCO/OH ratios tend to increase the gel content of the network and could also be used to further modulate the mechanical properties of the network. Detailed investigations of the influence of the NCO/OH ratio on the properties of such PU are beyond the scope of this study and will be reported elsewhere.

Characterizations. To analyze the lignin oligomers, a Shimadzu gel permeation chromatography (GPC) system was used. ^{31}P NMR spectra were recorded at room temperature on a Varian Inova 400 spectrometer using a 5 mm probe. The lignin−hydroxyl content determination is described in the Supporting Information. 2D ^{1}H−^{13}C heteronuclear single quantum coherence (HSQC) spectra were recorded in a Bruker advanced 500 MHz spectrometer equipped with a PABBI probe. The thermal phase transitions in the lignin oligomers were investigated using TA Discovery DSC 250. The sulfur content measurements were performed with the vario EL cube element analyzer (Elementar) (procedure in the Supporting Information). A Thermo Fischer FTIR i10 (Nicolet series)

https://dx.doi.org/10.1021/acs.biomac.0c00927
Biomacromolecules 2020, 21, 4135−4148

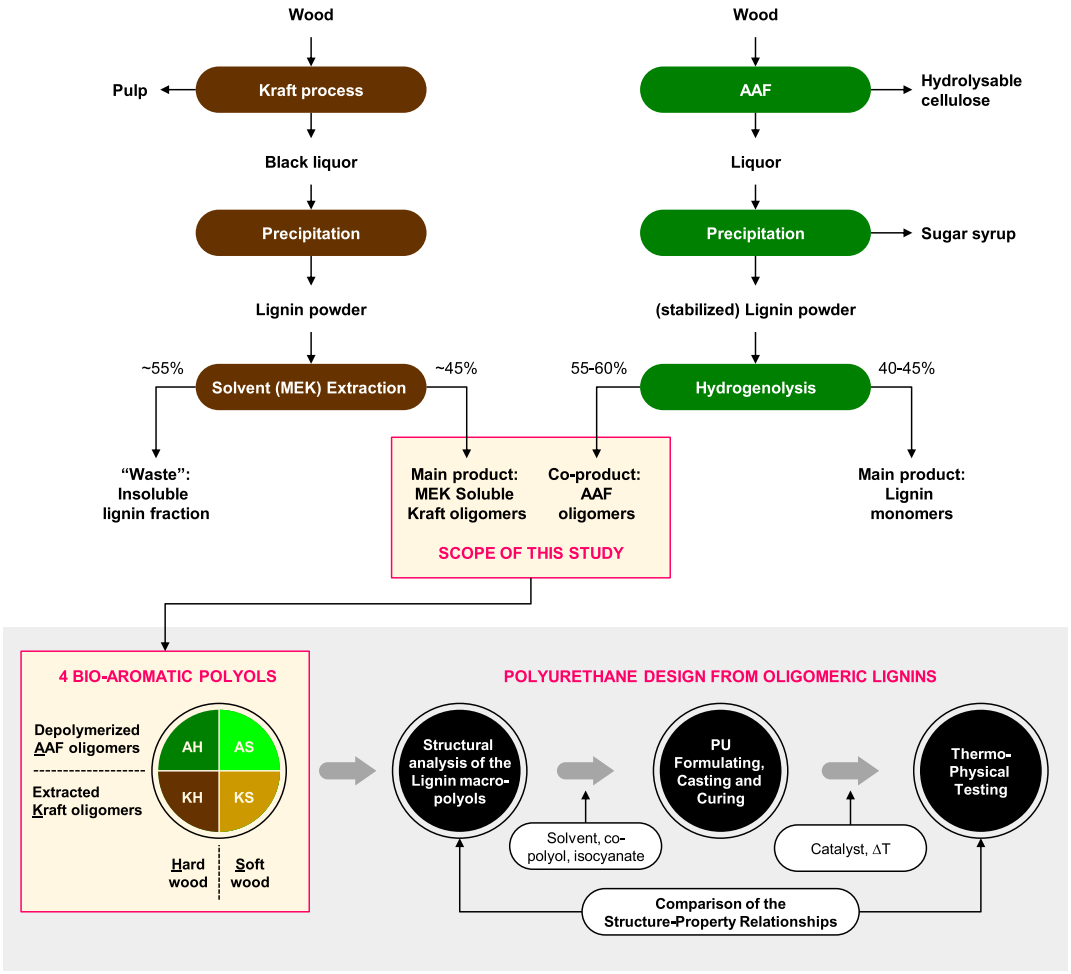

Figure 1. Scheme of the approaches explored in this study highlighting the four types of oligomeric lignins obtained via two biorefining processes (aldehyde-assisted fractionation process vs Kraft process) and different botanical origins (hardwood vs softwood) and the subsequent design and characterization of lignin-based polyurethane materials. The indicated yields are typical for hardwoods.

spectrometer was used in the attenuated reflectance (ATR) mode fitted with a diamond crystal. A TA Instruments Discovery Series DMA 850 dynamic mechanical analyzer and an Instron tensile testing machine (model 2412) were used to test the thermomechanical properties of the polyurethane films. Scanning electron microscopy (SEM) of cryo-fractured polyurethane specimens was performed with a Jeol JSM6340F microscope, and the XRD patterns were obtained with a diffractometer (Empyrean, Malvern Panalytical, United Kingdom). Complete description of the measurement protocols and characterizations are provided in the Supporting Information.

RESULTS AND DISCUSSION

Biorefining of Lignin Oligomers. We used two biorefining processes (Kraft and AAF) and two types of feedstocks which resulted in four oligomeric fractions that were used in subsequent PU synthesis and characterization (Figure 1).

The overall AAF biorefining process is depicted on the right side of Figure 1. One of its main features is the addition of aldehydes during an organosolv-like pretreatment that has been reported to efficiently protect the native-like lignin structure during its extraction from biomass.[29,31] By preserving the cleavable ether bonds and avoiding the formation of recalcitrant carbon−carbon linkages, this process allows the following lignin hydrogenolysis to reach near-theoretical yields of monomers based on ether cleavage (around 40−50% of Klason lignin for a hardwood and 20−30% of Klason lignin for a softwood).[32] In the first step, biomass is processed with an organic solvent, an acid, and an aldehyde. Lignin is stabilized while being solubilized, and hemicellulose is depolymerized into soluble monomeric carbohydrates. Cellulose remains as a solid which is recovered by filtration.[30] Lignin is recovered from the liquor through antisolvent precipitation and filtration. A concentrated syrup containing mostly hemicellulose-derived products can be obtained after removing the solvent from the liquor. The most abundant product in the syrup is xylose, stabilized with two equivalents of aldehyde when hardwood is used as the feedstock.[33] Lignin is depolymerized through metal-catalyzed hydrogenolysis to obtain monomers (45−50 mol % for hardwood and around 20 mol % for softwood)[31] and an oligomeric fraction. If monomer applications in chemistry have been extensively studied, the potential of the oligomeric fraction remains largely underexplored to date, despite few pioneering papers reporting the synthesis of epoxy bioresins from lignin oligomers obtained via AAF-related depolymerization processes such as lignin hydrogenolysis[34] or acid hydrogenolysis.[35]

The Kraft technology (Figure 1, left side) has been optimized for the industrial production of cellulosic Kraft pulp, which results in a worldwide production of around 70 Mtons/year of lignin-rich byproducts. In this process, wood is

https://dx.doi.org/10.1021/acs.biomac.0c00927
Biomacromolecules 2020, 21, 4135−4148

cooked at high temperature (170 °C) with hydrogen sulfide and hydroxyl anions in order to cleave the main lignin backbone consisting mainly of aryl ether bonds. Under such severe conditions, many side reactions such as the introduction of sulfur-based groups, the production of formaldehyde, the creation of new linkages including several interunit C−C linkages or stilbene-like structures, and the condensation of aromatic rings occur. In order to obtain better defined Kraft oligomers, we have chosen to perform pre-extraction using MEK (see details of the extraction process in the Supporting Information). As the botanical origin of the plant is known to influence the composition of the lignin, we have chosen to additionally consider the botanical origin of the lignin (hardwood vs softwood) as an additional parameter in this study.

In the rest of this study, the MEK-extracted oligomers derived from commercial hardwood and softwood Kraft lignin will be called KH and KS, respectively, while the hardwood and softwood AAF depolymerized oligomers will be called AH and AS, respectively. All oligomers were recovered in the powder form, with the AAF specimens displaying substantially lighter colors than their Kraft counterparts (Figure 2).

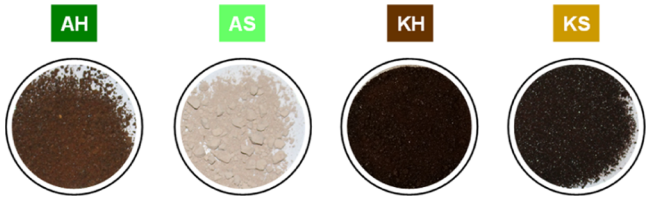

Figure 2. Physical appearances of the AAF oligomers AH and AS and of the Kraft-extracted oligomers KH and KS lignin oligomers (note the lighter colors of the AH and AS).

Characterization of the Lignin Oligomers. Here, a complete characterization of the oligomers (AH, AS, KH, and KS) was undertaken, with the final objective of establishing structure−property relationships between the molecular structures of lignin and the physical properties of PU materials. The molecular weight of the four oligomers was determined by GPC (Figure 3). All oligomers had comparable molecular weights with Mn values of around 1000 g/mol, except the AH specimen which displayed a slightly lower value (Mn = 803 g/mol) and thus the lowest Tg (Table 1). The fact that the four oligomers selected in this work displayed comparable molecular weights is an important parameter for the subsequent polyurethane design. In fact, this will reduce the potential effects of molar mass on the properties of the final thermoset resins. Consequently, any differences in thermo-mechanical properties of the PU resins are expected to correlate with molecular structure differences between the PU precursors (including the molecular structures of the lignins).

Quantitative ^{31}P NMR is the technique of choice to determine the different types of hydroxyl groups present in lignin.[36] 2-Chloro-4,4,5,5-tetramethyl-1,3-2-dioxaphospholane (TMDP) selectively reacts with the OH groups present in lignin, and the derivatized lignin (Figure 4b) can be analyzed by NMR (Figure 4a).

Aliphatic OH values were around 1 mmol/g for all the lignins except for AS, which was almost 2 units higher. The phenolic OH values showed a higher number for extracted lignins rather than for depolymerized lignins. In contrast, the distribution of condensed versus uncondensed phenolics is source-dependent. Softwood lignin contains mainly guaiacyl units (Figure 4b R = H), whereas hardwood lignin contains both guaiacyl and syringyl units (R = OCH_3). Therefore, condensed phenolic content is higher in hardwoods than in softwoods but both softwood and hardwood lignins contain condensed guaiacyl units (R ≠ H, OCH_3). In such a case, R can be another unit connected by β-5′, 5−5′, or 4-O-5′ linkage. It is important to note that condensed guaiacyl units and syringyl units appears in the range 144.5−140.2 ppm in ^{31}P NMR spectra (Figure 4a), and therefore, both are accounted as condensed phenolics (Figure 4b). Finally, carboxylic acid groups are barely present in depolymerized native lignin but significantly present in extracted Kraft lignin. This has been explained by the oxidation of aliphatic OH groups taking place during pulping.[37] Despite the difference in hydroxyl distribution, the total OH value of all the fractions was similar, around 6.5 mmol/g. AH was an exception, with less than 5 mmol/g.

To further characterize the oligomers' structure, we used the semiquantitative technique 2D ^{1}H−^{13}C HSQC. Cross peaks corresponding to lignin substructures/linkages were assigned by comparison with previous work.[22,31,38] The ratio of the different linkages present in lignin samples and the aromatic unit ratio (S/G/H) were determined, both expressed per 100Ar units (Table 2, see the Supporting Information for details on the calculation).[39,40] Within the aromatic region, we clearly observed the difference between softwoods (AS and KS) and hardwoods (AH and KH) because spectra from SW lacked S unit signals as gymnosperms (softwoods) contain exclusively guaiacyl units.[41] Among all the detected signals (Table 2), we mainly focused on the β-O-4′ (A), β−β′ (pinoresinol, B), β-5′ (C), and dibenzodioxocin (E) linkages because these substructures were present in every lignin. For AH and AS, we also paid attention on β-O-4′ isobutyraldehyde substituted units (iBA). The aliphatic region (δ_C/δ_H 50−90

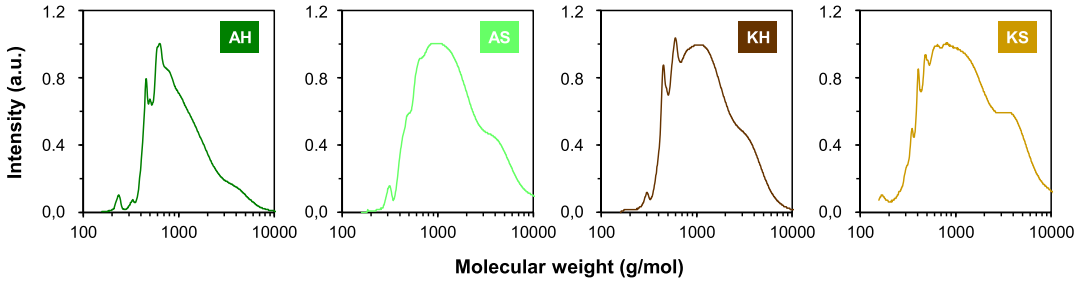

Figure 3. GPC analysis of the four oligomeric lignins considered in this work.

https://dx.doi.org/10.1021/acs.biomac.0c00927
Biomacromolecules 2020, 21, 4135−4148

Table 1. Analytical Characterization of the AAF and Extracted Kraft Oligomers

name	botanical origin	Mn[a] (g/mol)	Mw[a] (g/mol)	Đ[a]	total OH[b] (mmol/g)	f[c]	Tg (°C)[d]	sulfur (wt %)
AH	beech	803	1600	1.9	4.85	3.89	53	0.17
AS	spruce/pine	1050	1940	1.8	6.38	6.70	79	bdl[e]
KH	eucalyptus	943	1590	1.6	6.22	5.87	81	1.93
KS	pine	892	1940	2.1	6.74	6.01	62	1.75

[a]Determined by GPC (Mn: number average molecular weight, Mw: number average molecular weight, and Đ: polydispersity index). [b]Sum of phenolic, aliphatic, and carboxylic hydroxyl groups determined via ^{31}P NMR. [c]f = average functionality (average number of OH groups per oligomer, calculated with f = Mn × [total OH]/1000). [d]Tg: glass transition temperature determined by DSC. [e]Sulfur content determined by elemental analysis (bdl: below detection limit).

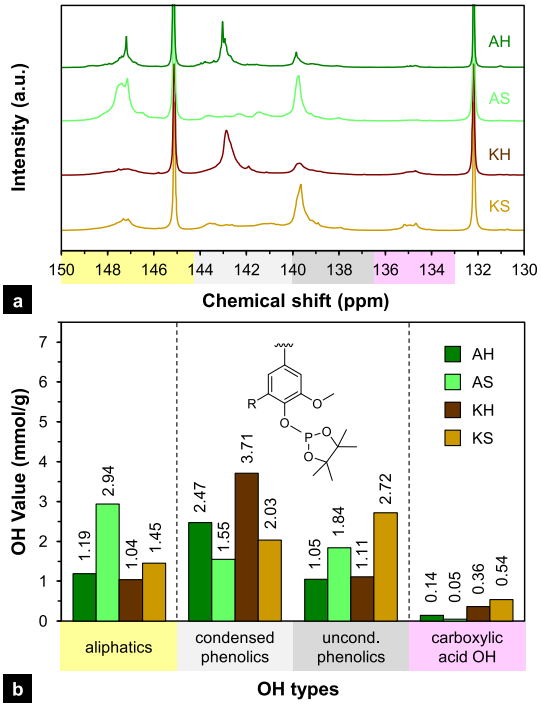

Figure 4. (a) ^{31}P NMR spectra for AH, AS, KH, and KS oligomers and (b) histograms summarizing the integrations. The inset shows the molecular structure of a phosphorylated phenolic hydroxy group.

Table 2. Semiquantification of the Aromatic Unit Ratio (S/G/H) and of the Most Occurring Lignin Interunit Linkages (Expressed per 100Ar Units)

oligomeric lignin	AH	AS	KH	KS
G ratio	24.1	100	23.5	95.7
S ratio	75.9		76.5	
H ratio				4.3
β-O-4′ (A)	1.6	5.4	2.8	3.2
β–β′ (B)	4.6	5.8	3.9	3.3
β-5′ (C)	0.3	8.1	0.2	1.4
γ-hydroxypropyl end groups (D)	4.7	9.6	0.9	2.9
dibenzodioxocin (E)	2.6	2.0	1.6	1.4
α-hydroxy acids (F)			0.7	1.8
isobutyraldehyde substituted units (iBA)	1.3	2.7		
stilbene (L)			1.9	3.8

ppm/2.5–5.5 ppm) and aromatic region (δ_C/δ_H 100–130 ppm/6–8 ppm) were integrated to make the calculations.

As reflected in Table 2, the β-O-4′ linkage (δ_C/δ_H, 71.1/4.77, C_α-H_α, A_α→ signal used for integration) is present in every sample we studied but not in the same ratio. We observed that softwood oligomers contain a higher amount of such substructures than hardwood oligomers. β–β′ bonds (δ_C/δ_H, 85.0/4.62, C_α-H_α, B_α) and dibenzodioxocin (δ_C/δ_H, 81.1/4.76, C_β-H_β, E_β) were also present in every sample but in a higher ratio in AAF depolymerized oligomers. Because of the oligomeric depolymerized nature of AH and AS, a higher ratio of 4-hydroxy propyl end groups (δ_C/δ_H, 34.4/1.70, C_β-H_β, D_β) were found in AH and AS than in KH and KS. We also noted the quasi absence of β-5′ structures (δ_C/δ_H, 86.6/5.46, C_α-H_α, C_α) in HW (only seen at a low contour level).

What was especially remarkable was the difference in the ratio of the β-5′structure between KS and AS. The fact that AS has the higher ratios of β-O-4′, β-5′, and 4-hydroxy propyl end groups is in full agreement with results obtained from ^{31}P NMR. The more abundant these structures are, the more aliphatic OH were detected by quantitative ^{31}P NMR. In this context, the trend of aliphatic OHs present in the different oligomers (KH < AH < KS < AS, determined by ^{31}P NMR) perfectly matched with the semiquantification of linkages bearing such a functionality (β-O-4′, β-5′, 4-hydroxy propyl end groups, dibenzodioxocin, and α-hydroxy acids), following therefore the same trend (KH < AH < KS < AS; sum of 2 × A + C + D + E + F values, obtained by 2D analysis). Finally, signals corresponding to β-O-4′ isobutylidene acetal-protected linkages (δ_C/δ_H, 102.1/4.66, C1–H1, iBA1) in AH and AS lignins were analyzed. Ratios of 2.7 and 1.5% for AS and AH, respectively, were determined. This ratio was higher for the AS sample, following the same trend as for β-O-4′.

In addition, other linkages/substructures were present only in some of the lignin(s) studied. For instance, β–β′ (secoisolariciresinol, **I**) appeared only in KS with a ratio of 1.5%. Stilbene units (**L**) were detected in both KS and KH. However, enol ether structures (**K**) were only detected in KS lignin, in a very low contour level and a ratio of 0.36 per 100Ar units. α-Hydroxy acid substructures (**F**) (δ_C/δ_H, 73.6/4.43) are present in KS and KH but were not found on AS or AH. This analysis highlights not only the differences in lignin (sub)structures between hardwood/softwood lignins but also between Kraft-fractionated and AAF-depolymerized lignins.

Enhanced Solubility of AAF Oligomers. Lignin solubility is an important criterion for the design of polyurethane materials as it facilitates the incorporation of the lignin segments into the polymer matrix and allows the isocyanate groups to react with the exposed OH moieties.[13] In addition, dissolving the PU precursors in a common solvent is a prerequisite step in several applications such as coatings. The solubility of the AH, AS, KH, and KS oligomers and of the two unfractionated Kraft lignins (hardwood and softwood) have been qualitatively screened via solubility tests in a selection of six solvents of various solubility parameters, namely, diethyl ether, ethyl acetate, MEK, tetrahydrofuran, dichloromethane, and ethanol, as displayed in Figure 6.

https://dx.doi.org/10.1021/acs.biomac.0c00927
Biomacromolecules 2020, 21, 4135–4148

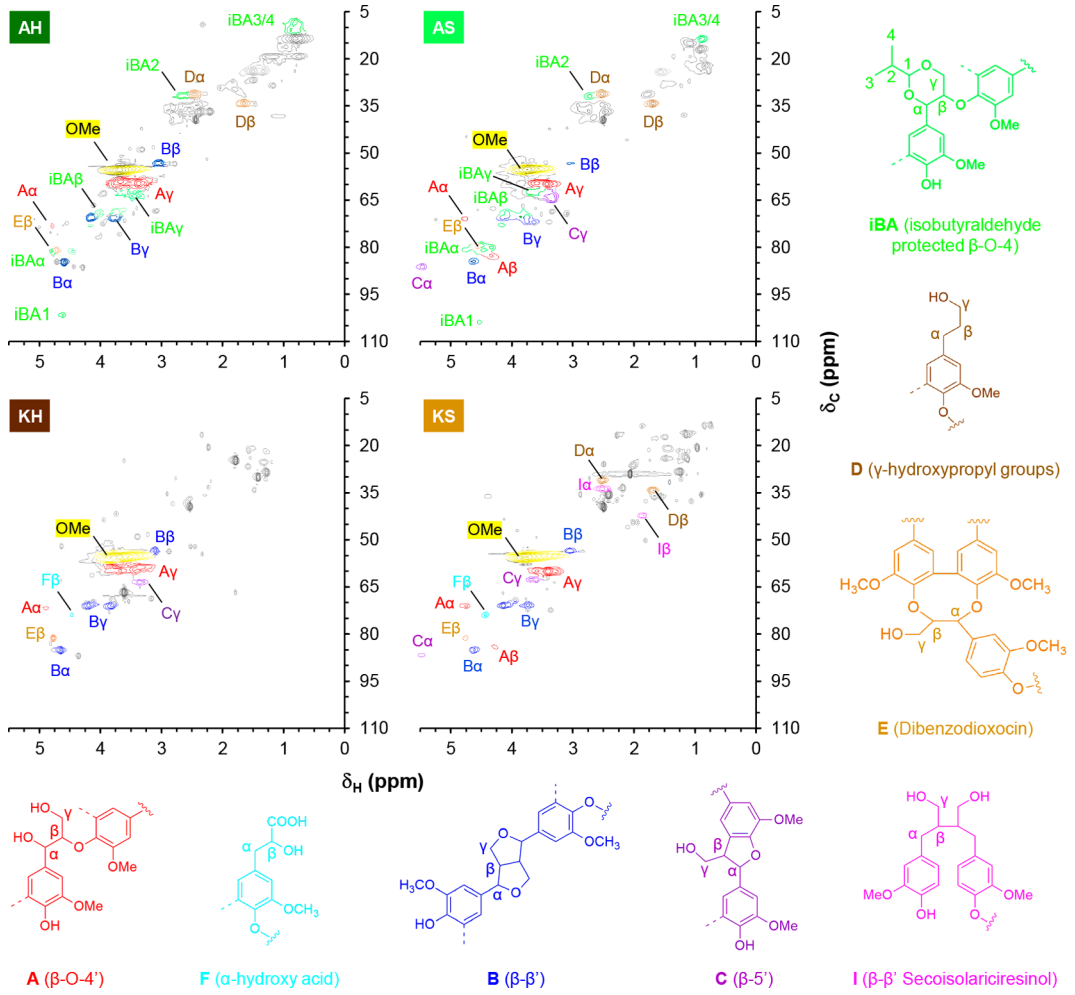

Figure 5. 2D $^{1}H-^{13}C$ HSQC NMR spectra for AH, AS, KH, and KS oligomers. δ_H, proton NMR chemical shift (in parts per million); δ_C, carbon NMR chemical shift (in parts per million). The aromatic regions are shown in Figure S1.

The two unfractionated Kraft lignins showed very poor solubility in all solvents, except in THF that could almost completely dissolve the softwood Kraft lignin sample. The very poor solubility of Kraft lignin in solvents of lower polarity (such as EtOAc) was not a surprise because a relatively high solubility parameter of 24.6 has been reported for softwood Kraft lignin.[42,43] One consequence for the design of Kraft lignin-based PU is the requirement for exotic solvents of very high polarity such as dimethylformamide (DMF) or dimethylsulfoxide (DMSO) to solubilize the lignin.[44] These solvents are not ideal in an industrial context because of their high boiling point and toxicity. The pre-extracted KH and KS samples display improved solubility compared to their unfractionated mother lignin. Both samples are quite soluble in THF and also redissolve in MEK (which was used as an extraction solvent). However, the solubilities of KH and KS are still quite limited in the other solvents.

In comparison, the AAF oligomers display much better solubilities. Especially, AH quickly (within few minutes under gentle shaking) and completely solubilizes in EtOH, DCM, THF, MEK, and EtOAc and shows the highest solubility of the four oligomers in Et_2O. AS could also almost completely (~80%) dissolve in all the solvents except Et_2O. Overall, Figure 6 demonstrates the versatility of the AAF oligomers to be formulated in a variety of common organic solvents and suggests that these oligomers could also be better integrated in polymer matrices of various polarities.

Polyurethane Design and Network Development. Our polymer design is based on a three-component PU system where the lignin oligomers are playing the role of the hard segments, a copolyol is bringing flexibility and lowers the Tg, and an aliphatic trifunctional isocyanate is added as the cross-linking agent. Concerning the choice of the lignin copolyol, many studies so far have concentrated on polyethylene glycol (PEG) because it is the only copolyol that has the ability to partly solubilize Kraft lignin by disrupting the strong lignin–lignin interactions. However, PEG is not always an ideal component for material design because it is quite hygroscopic and has a relatively high Tg compared to other polyethers. Instead, we have opted for polytetrahydrofuran (PTHF), a widely applied and highly flexible polyether polyol used in various applications such as Elastane. The lignin oligomers were introduced in polyurethane (PU) formulations with various degrees of substitutions (10–100%) in comparison to the PTHF copolyol. Thermoset lignin PU was then obtained by cross-linking of the polyol mixtures with an aliphatic polyisocyanate based on a hexamethylene diisocyanate trimer (Desmodur N3600), which is used as a hardener for PU coatings and elastomers with excellent weatherability and resistance properties (see molecular structures on Table 3).

https://dx.doi.org/10.1021/acs.biomac.0c00927
Biomacromolecules 2020, 21, 4135–4148

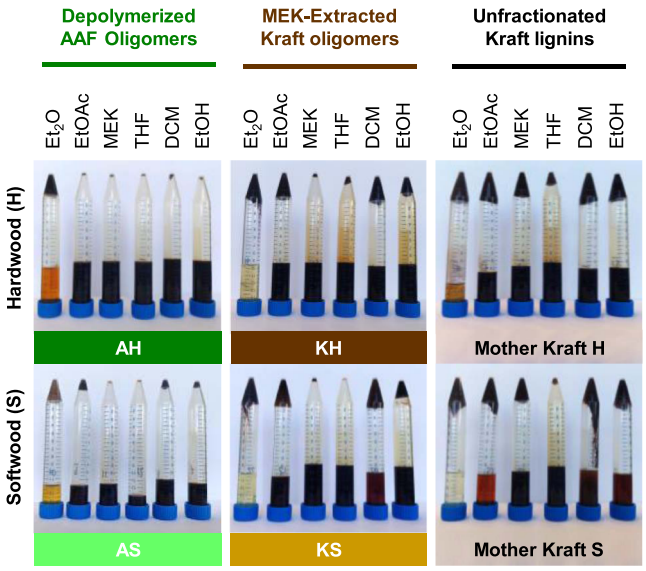

	Et_2O	EtOAc	MEK	THF	DCM	EtOH
δ_d	14.24	15.36	15.63	16.89	18.32	15.41
δ_p	3.85	5.02	8.60	4.93	17.23	8.56
δ_h	5.37	8.47	4.73	6.08	3.54	18.51
δ_{total}	15.70	18.24	18.45	18.62	25.40	25.56

Figure 6. Solubility screening (at 100 mg/mL) of AH, AS, KH, and KS oligomers in a selection of six organic solvents featuring various solubility parameters. Similar tests have also been performed with the unfractionated Kraft lignin. δ_d, δ_p, δ_h, and δ_{total} represent the dispersive, polar, hydrogen bonding, and total contributions, respectively, of the Hansen solubility parameters of the selected organic solvents. Et_2O: diethyl ether; EtOAc: ethyl acetate; MEK: methyl ethyl ketone; THF: tetrahydrofuran; DCM: dichloromethane; EtOH: ethanol.

In order to ensure the complete solubilization of the four lignin oligomers in a common solvent, the pre-extraction solvent of KH and KS (MEK) was further used as the solvent for formulating the AHPU, ASPU, KHPU, and KSPU materials (see nomenclature in Table 3). All PU materials reported in this work were synthesized with an NCO/OH ratio of 0.9 (Table 3) based on the total (phenolic + aliphatic) OH value determined by ^{31}P NMR (Table 1). After mixing the catalyst, lignin oligomers, and the copolyol in MEK, isocyanate was added. The reaction mixture was stirred at 40 °C for 1 h, poured into a Teflon mold, and then left to evaporate overnight. The resulting lignin PU films were then cured for 6 h at 100 °C.

The slight excess of OH groups (slight lack of NCO groups) has been chosen considering that the lignin molecules possess intrinsically a quite high OH functionality and also assuming that not all of these OH groups might be able to react with NCO groups. This NCO/OH ratio of 0.9 represents an average value compared to previous lignin PU reported in the literature, in which a wide range of ratios has been reported ranging from 0.2 for high lignin-content coatings[45] to 2.1 for flexible transparent lignin films.[46]

The completion of the reaction between the polyols and NCO groups was monitored using Fourier transform infrared (FTIR) spectroscopy. For all the films produced, the disappearance of the N=C=O stretching signal of the isocyanate at 2260 cm^{-1}, which is inherent to the formation of

Table 3. Explanation of the Bioresin Nomenclature, Molecular Structures of the PTHF Copolyol and of the Trimerized HDI (Hexamethylene Di-isocyanate) Cross-Linker, and Selected Examples of PU Formulations (With a Molar Ratio of r = [NCO]/[OH] = 0.9)

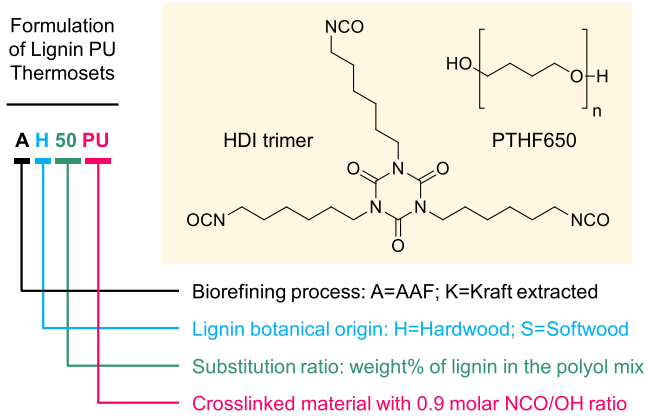

	formulation wt % (mol %)		
specimen	lignin	PTHF	HDI trimer
AH40PU	24.3 (26.9)	36.4 (25.5)	38.6 (47.2)
AH60PU	35.1 (36.9)	23.4 (15.5)	40.7 (47.2)
AH80PU	45.2 (45.3)	11.3 (7.1)	42.7 (47.2)
AH100PU	54.6 (52.4)	0	44.6 (47.2)
AS80PU	40.4 (46.8)	10.1 (5.6)	48.6 (47.2)
KH80PU	40.9 (46.7)	10.2 (5.8)	48.0 (47.2)
KS80PU	39.4 (47.1)	9.9 (5.4)	49.8 (47.2)

urethane linkages, was observed. As shown in Figure 7a, the broad OH stretching signal present in the original AH lignin (3421 cm^{-1}) was ultimately absent in the films AH40PU and AH80PU and resulted in a new signal centered at 3365 cm^{-1} ascribed to the hydrogen-bonded N−H stretching signal of the urethane bond. These results indicated that the OH groups of the different lignin oligomers readily cross-linked with the hexamethylene diisocyanate.

FTIR spectroscopy can also be used to study the chemical structure of the lignin PUs with characteristic bands in the spectral region 1000−1800 cm^{-1}. At 1680 cm^{-1}, an intense band correlating to the carbonyl moiety in the urethane bond appeared, demonstrating the formation of PU. The C−N stretching vibration band at 1460 cm^{-1} is observed in addition to the typical aromatic skeleton vibrations in lignin around 1500 cm^{-1}. The less intense signals in the PU spectrum at 1112 and 1211 cm^{-1} may be attributed to the C−O deformation of terminal hydroxyl groups and the C−O−C stretching.[23,44,45,47]

These results show that the lignin oligomers are indeed covalently linked to the isocyanate via urethane bonds to yield a cross-linked material. The gel content (defined as the weight ratio of the dried polymer network to that of the polymer before washing with a good solvent such as DMF) analysis for several LPU networks (Figure 7b) confirmed that the lignin is covalently incorporated in the polyurethane networks with gel fractions above 90%. AHPU networks display lower gel contents than the other systems, which can be attributed to the lower functionality of the AH oligomer (Table 1). For a given system, the gel content increases with the weight % of lignin in the polyol mix, highlighting the cross-linking effect of

https://dx.doi.org/10.1021/acs.biomac.0c00927
Biomacromolecules 2020, 21, 4135−4148

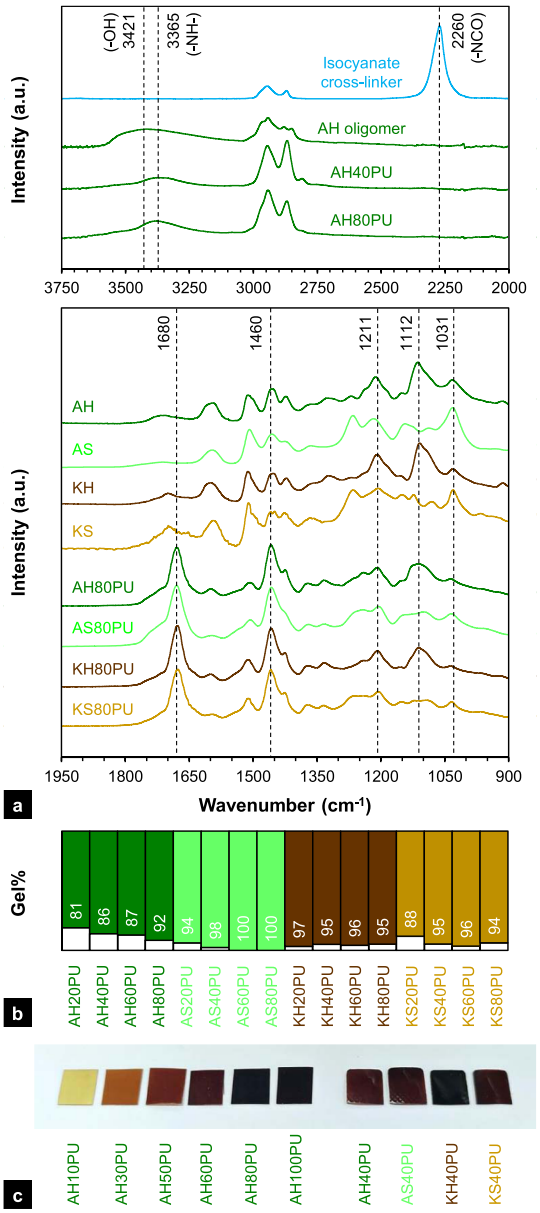

Figure 7. (a) Top: FTIR spectra demonstrating the full curing of AH40PU and AH80PU; bottom: fingerprint region of AH80PU, AS80PU, KH80PU, KS80PU, and of the corresponding oligomers AH, AS, KH, and KS; (b) gel fractions (*insoluble fraction in DMF*) for several LPU networks. White bars represent the soluble fractions (sol % = 100 − gel %), while filled bars and labels indicate the gel fractions; (c) images of a selection of amber-colored lignin PU networks (dimension: 10 × 10 mm and thickness: 350 μm).

the lignin segments. The soluble fraction in DMF is most probably due to lignin residuals.

The cured PU networks were obtained as amber-colored films of various flexibilities and transparency levels (Figure 7c). At comparable lignin ratios, materials derived from AAF oligomers (AH and AS) tend to be lighter in color than their Kraft-derived counterparts, an observation that could be correlated to the lighter colors of the starting oligomers (cf. Figure 2). For instance, AH100PU networks still display some level of transparency (despite its black appearance on Figure 7c), while KHPU networks are already completely black/opaque with only 30% of lignin.

Dynamic Mechanical Analysis at Small Strain. The dynamic mechanical analysis of the LPU (lignin polyurethane) networks has been characterized by the temperature dependencies of the storage modulus E' and the loss modulus E'' determined in tensile mode experiments with sinusoidal signals in the linear viscoelastic regime. The evolution of E' and of the loss factor tan δ (tan $\delta = E''/E'$) as a function of temperature is given for AH60PU and AH80PU in Figure 8a.

All DMA curves are characterized by a single relaxation step dominating the whole spectrum. The maximum of tan δ corresponds to a segmental relaxation of polymeric units near the glass transition temperature and is therefore a short-range phenomenon involving only few monomers. Here, we note Tα as the characteristic temperature associated with this relaxation. At temperatures well below Tα, the molecular motions are frozen and the networks are in a glassy state. On the other hand, above Tα, the macromolecular chains become increasingly mobile and the networks are in a rubbery state characterized by an E' plateau (noted here E_P'), in accordance with the classical theories of rubber elasticity.[48,49]

The viscoelastic windows for AHPU, ASPU, KHPU, and KSPU systems have been constructed by plotting Tα against E_P' for each set of networks (Figure 8b). Independent of the lignin type used for the synthesis, the values of Tα and E_P' systematically increase with the amount of lignin in the LPU material. This increase can be explained both by the molecular structure of lignin-containing rigid bioaromatic rings and by various linkages (see structures on Figure 5) which are intrinsically less mobile than the ultraflexible PTHF segments. On the other hand, with the OH functionality being more important in lignin (see f values for each oligomers in Table 1, to be compared to $f = 2$ for PTHF), we assumed that the overall cross-linking density of the network will increase because of the higher branching/cross-linking induced by the lignin repeating units.[50,51] The level of storage modulus E' in the rubbery plateau region provides an indication on the cross-linking density of the network (noted ν_C). In the framework of the ideal network law (i.e., assuming that all chains are elastically active and neglecting network defects such as loops and dangling chains), ν_C can be estimated by the equation $E_P' = 3\cdot(\nu_C)\cdot R\cdot T$, where ν_C is expressed in moles of elastically effective network chains per cm^3, T is the absolute temperature corresponding to the E_P' value, and R is the gas constant.[48] From the abovementioned equation, an increase in ν_C is expected to induce a proportional increase in E_P', such as the one observed in Figure 8b. The results of the gel content analysis (Figure 7b) also confirmed this hypothesis because the percentages of the gel fraction (which is correlated to the cross-linking density ν_C) tend to increase with the percentage of lignin in the resin.

Interestingly, different slopes could be observed in Figure 8b for the PU materials obtained from AAF oligomers (both AHPU and ASPU) and the ones obtained from Kraft-extracted oligomers (both KHPU and KSPU). Especially, for a lower amount of lignin, AHPU and ASPU materials display inferior E_P' values than KHPU and KSPU networks. In this case, the ideal network law would again suggest that KH- and KS-based PU are more cross-linked than their AH- and AS-based counterparts. Although it is true for the AHPU networks which possess a lower cross-linking density because of the lower functionality of the AH oligomers, it is not the case for the ASPU networks which display very high gel content (Figure 7b). Therefore, in this specific case, the lower E_P' values of

https://dx.doi.org/10.1021/acs.biomac.0c00927
Biomacromolecules 2020, 21, 4135−4148

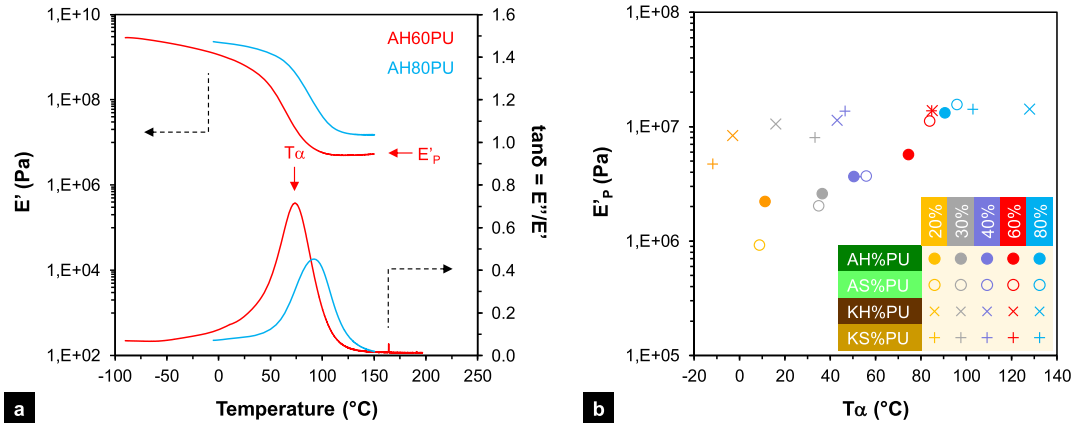

Figure 8. (a) DMA profiles of AH60PU and AH80PU networks showing the temperature evolution of the elastic modulus E' and of the loss factor tan δ. E_P' and Tα represent the dynamic modulus in the rubbery plateau region and the temperature at tan δ max, respectively. Black dotted arrows indicate the relevant axis for the associated curves; (b) viscoelastic windows (E_P' vs Tα) for AHPU, ASPU, KHPU, and KSPU systems. Note the different slopes observed for the A(H/S)PU networks vs K(H/S)PU networks.

ASPU networks could not be attributed to a difference in cross-linking density, and the ideal network law does not explain the observed discrepancies. An alternative hypothesis could be formulated by considering the molecular structure of the lignin segments. The AAF oligomers (AH and AS) possess a more native and flexible lignin structure (see Table 2 and Figure 4), while the Kraft-extracted oligomers contain multiple carbon−carbon linkages bringing rigidity to the lignin backbones. For lower lignin content, the differences E_P' could therefore be attributed to the intrinsic nature of the lignin oligomers rather than to the cross-linking density. An important implication is that the AAF oligomers could allow the design of a wider range of PU materials, including for applications requiring a lower modulus in the rubbery plateau.

For higher loadings of lignin, this discrepancy in E_P' values between AAF-based PU and Kraft-extracted PU gradually diminish, and ultimately, the E_P' values at 80% lignin become quite similar for the four materials. This suggests that in the case of higher lignin contents, the mechanical properties in the rubbery state are more largely dominated by the overall cross-linking density of the network (and the associated restricted mobility of polymer chains around cross-links) rather than by the intrinsic nature of the lignin backbones.

Morphological Insights. Some morphological insights can be deduced from the bulk thermomechanical profiles of the materials. In particular, the shape and width of the tan δ peak can reveal some insights into the homogeneity of the PU networks. To this end, we measured the full width at half-maximum (noted fwhm) of the tan δ peaks for each set of networks (Figure S2a). Overall, the AAF-based networks AHPU and ASPU display relatively uniform tan δ peaks associated with fwhm values of around 60 °C. This value tends to be higher than the fwhm values commonly observed with well-defined and more polydisperse synthetic polymers, suggesting that our lignin PUs all display some level of inhomogeneities that could be associated with diverse relaxation phenomena attributed to the various components of the macromolecular structure (such as the rigid bioaromatic segments, the flexible PTHF segments, or the various potential network defects such as dangling chains, loops, or the sol fraction).[52] A very different DMA profile was observed with KSPU networks with low lignin contents (typically from 10 to 50% polyol substitution). In this case, much higher fwhm values of up to 130 °C were observed (Figure S2c), and the associated tan δ peaks display a clear bimodal distribution (Figure S2b). These observations suggest that phase separation occurs to some extent in KSPU networks. In the case of PU synthesized from the unfractionated Kraft lignin, the current synthetic protocol leads to completely inhomogeneous and phase-separated materials.

The microscale morphology of cryo-fractured PU specimens was studied using SEM (see typical images in Figure 9) for

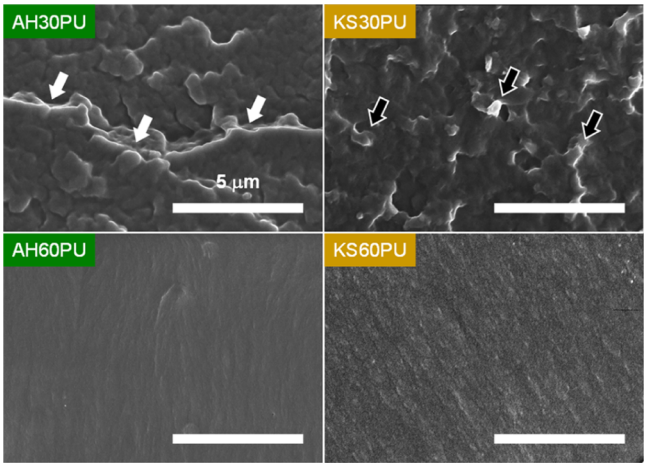

Figure 9. SEM pictures of cryo-fractured AHPU and KSPU networks with two different lignin ratios. The white arrows indicate signs of a ductile-like fracture, whereas the black arrows highlight signs of brittle fracture around (phase segregated) lignin-rich domains.

AHPU and KSPU networks with substitution ratios of 30 and 60%, respectively. Under these conditions, AH30PU displays a ductile fracture pattern and popcorn-like spherical structures of around 100 nm that could suggest the presence of slightly more cross-linked domains within the material.

At similar lignin content, the KS30PU network presents a very different and more brittle-like fracture pattern, in which some phase-separated (lignin-rich) domains are clearly visible. Visually, KS30PU is not even fully transparent, an observation that indirectly confirms the formation of larger phase-segregated domains able to partially diffract light. Similar to the higher solubility of the AH and AS oligomers in organic

https://dx.doi.org/10.1021/acs.biomac.0c00927
Biomacromolecules 2020, 21, 4135−4148

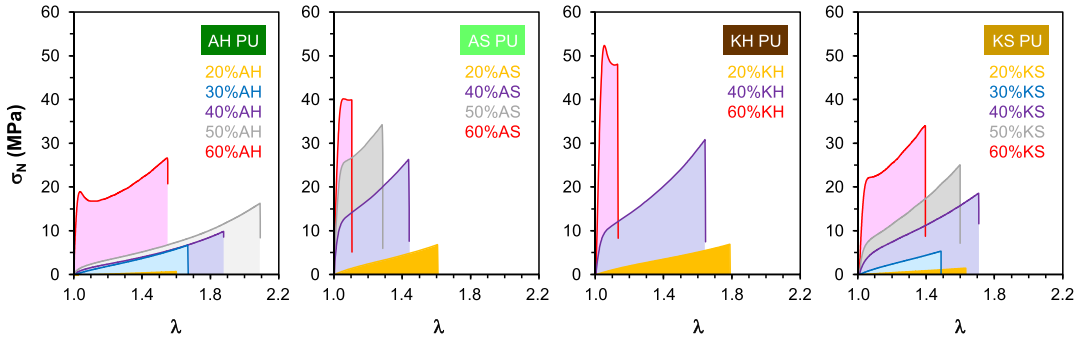

Figure 10. (a) Representative stress–strain profiles (stress σ_N as a function of the elongation λ) for the four series of LPU biomaterials. The filled area below each curve represents the fracture energy (a measure of the toughness of the network). The tangent at small elongation provides the Young modulus. The Mooney representations of these tensile curves highlighting strain-hardening effects are shown in Figure S4. The elongation is a dimensionless parameter defined as $\lambda = l/l_0$, where l and l_0 are the stretched and initial lengths of the specimen, respectively. The λ values of 1.0, 1.4, 1.8, and 2.2 correspond to percent elongation values [with λ % = 100 × $(l - l_0)/l_0$] of 0, 40, 80, and 120%, respectively.

solvents, the more homogeneous morphology of the resulting AHPU and ASPU networks highlights the better compatibility of these AAF oligomers with the PU networks (for instance, copolyol PTHF has a solubility parameter of 18.3 $MPa^{1/2}$, and AH was found to be fully soluble in solvents of similar δ). In contrast, the more limited solubility observed with the KS oligomer will also alter its proper integration in the PU matrix. For higher lignin content (60%), AH60PU and KS60PU networks both display homogeneous morphologies, and the fractured networks display signs of brittle fracture.

Morphologies at an even smaller scale were investigated by X-ray diffraction techniques, which examine the long-range order produced as a consequence of short-range molecular interactions.[53] Figures S3 shows the XRD diffraction patterns of the AH and KS oligomers and of their respective AHPU and KSPU networks with various lignin contents (20–100% polyol substitution). The powder diffractograms of both AHPU and KSPU networks exhibits broad peaks at 2θ angles around 11.2, 20.5, and 43.0°. The two large Bragg peaks at 20.5 and 43.0° are similar for all the networks and represent the signature of the amorphous halo, which can also be found on the diffractograms of the oligomers.[54] In contrast, the peak at 11.2° could not be observed on the XRD pattern of the AH and KS oligomers and displays a strong dependency on the lignin content. This peak can therefore be assigned to the scattering from PU chains with regular interplanar spacing.[55] The proportional increase between the intensity of the 11.2° Bragg peak and the lignin content in the network can be associated with the specific fingerprint of the short-range order induced by the lignin segments within the polymer matrix and suggests the formation of a hard–soft block-copolymer network structure, in which lignin-rich nanoscale macromolecular clusters are interconnected via more flexible PTHF repeating units.

Morphologies at an even smaller scale were investigated by X-ray diffraction techniques, which examine the long-range order produced as a consequence of short-range molecular interactions.[53] Figures S3 shows the XRD patterns of the AH and KS oligomers and of their respective AHPU and KSPU networks with various lignin contents (20–100% polyol substitution). These powder diffractograms indicate that all the PU biomaterials are amorphous because of the absence of sharp scattering peaks. The two large Bragg peaks at 20.5 and 43.0° are similar for all the networks and represent the signature of the main amorphous halo, which can also be found on the diffractograms of the oligomers.[54] Especially, the peak at 20.5° (which is also predominant in the XRD patterns of the unformulated oligomers AH and KS) can be associated with the separation distance distribution of the lignin aromatic ring.[56,57] The intensity of the 11.2° Bragg peak is increasing with the lignin substitution ratio in the bioresin. As a higher lignin loading corresponds to a lower isocyanate content in the PU (see formulation Table 3), we hypothesize that the 11.2° peak corresponds to the separation distance distribution of urethane bonds.

Tensile and Ultimate Mechanical Properties. Although the dynamic mechanical properties at small strain provide insights into the structure of the lignin PU networks, they do not provide information related to their large-strain mechanical behavior and their ultimate properties. Therefore, tensile experiments are useful to provide this information. Representative stress–strain profiles of the four series of LPU materials are displayed on Figure 10, and the complete results with standard deviations can be found in Table S3.

For each set of networks, the tangent at low elongation gives an indication of the Young modulus of the material and increases with the lignin content. Notably, we studied how the specific molecular characteristics of each oligomer could affect the macroscopic tensile properties of the resulting PU materials. For instance, at similar lignin content, AHPU networks display lower modulus and higher elongation at break compared to ASPU networks. This observation can be attributed to the lower functionality of the AH oligomers (Table 1) which will lead to more open network structures possessing a higher molecular weight between cross-links. In contrast, AS oligomers display a higher functionality and will create denser networks with lower molecular weight between cross-links.[58]

Another peculiar behavior of some AHPU networks (such as AH30PU, AH40PU, and AH50PU) is the pronounced strain-hardening effect observed at high elongation. This pronounced non-linear stain-hardening behavior appears more clearly using the Mooney stress (σ_R) representation displayed in Figure S4, in which the measured stress is normalized by the expected behavior of a neo-Hookean rubber in uniaxial extension (with $\sigma_R = \sigma_N/[\lambda - (1/\lambda^2)]$).[59,60] In fact, the strain-hardening regions are now indicated by clear minimums in the $1/\lambda$ representation at high extension.[61] For conventional elastomeric systems such as natural rubber, such strain hardening is usually associated with strain-induced crystallization of the

https://dx.doi.org/10.1021/acs.biomac.0c00927
Biomacromolecules 2020, 21, 4135–4148

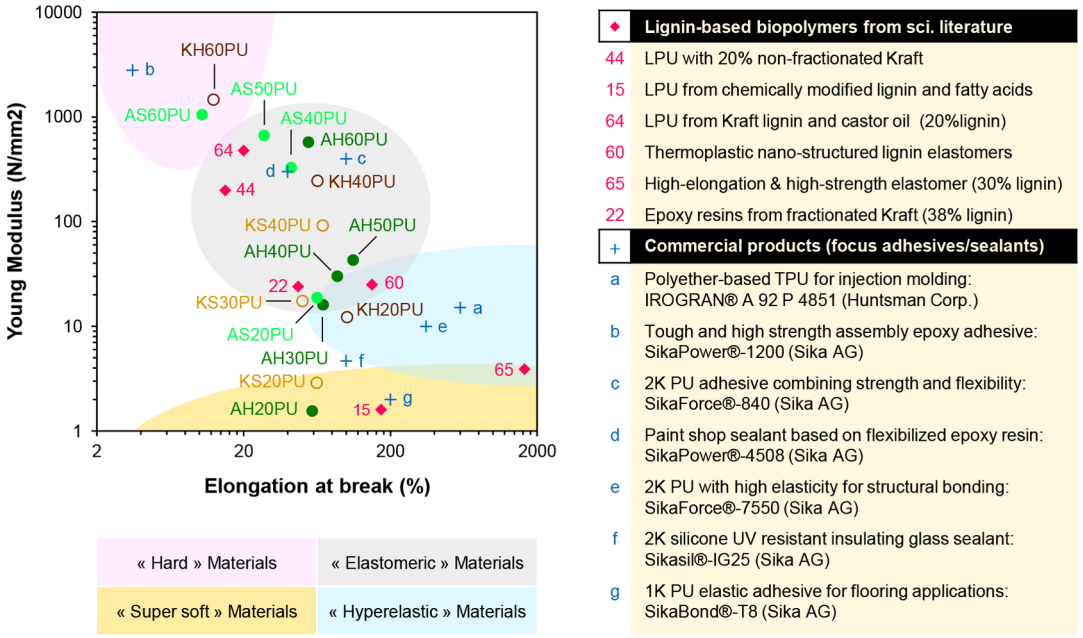

Figure 11. Ashby plot of Young's Modulus vs Elongation at break for the LPU materials developed in this work. The legend provides a selection of benchmarking references obtained from ("diamond" markers) lignin-based biopolymers reported in the scientific literature (the reference numbers correspond to the main reference list at the end of this article) and ("+" markers) commercial polymeric systems with a focus on adhesives and sealant products.

chains.[49] In our current study, this hypothesis is unlikely considering the amorphous nature of these lignin-based PU resins. For noncrystallizable systems, the upturn associated with strain hardening has also been explained by the limited chain extensibility of certain bimodal macromolecular networks in which more densely cross-linked nanoscale domains are connected via longer flexible chains.[59,62,63] This bimodal structure hypothesis could better fit with the hypothetical structure of a lignin PU network formed via the combination of two polyols of widely different characteristic (lignin oligomers and PTHF).

Benchmarking the Performances of Lignin PU Bioresins. An Ashby plot was constructed in Figure 11 by plotting the Young modulus against the elongation at break for each set of the lignin PU system. A schematic representation of common material archetypes was also superimposed in the figures, highlighting the domains covered by hard materials, elastomeric materials, hyperelastic materials, and soft materials. This Ashby plot reveals that the lignin PU resins developed in this work could cover a very wide range of properties. Several benchmarking references are also provided in Figure 11, including several lignin-based polymers from the scientific literature and a selection of commercial polymeric products.[15,22,44,54,60,64,65] Although the AAF lignin PU materials synthesized in this work were not yet optimized for any specific applications, their final properties were comparable to the properties of a selection of nonrenewable commercial materials from the adhesives/sealant market. Such materials could also be interesting in the field of (nano)composite materials, for instance, in the automotive markets.[66,67] This comparison highlights the potential of AAF oligomers to be integrated into various commercially relevant polymer systems upon further formulation.

At a similar lignin ratio, the lignin PU prepared from Kraft-extracted oligomers display overall comparable results as compared to the AAF-derived PU. However, it should be recalled here that the solvent-based PU synthetic protocol (using MEK as a solvent) has been designed in order to allow the synthesis of homogeneous materials from the Kraft-extracted oligomers. Changing the concentration or the type of solvent will induce pronounced phase separation within the Kraft-based materials, making any comparison with the AAF-derived PU irrelevant. In fact, this is drastically different for the AAF oligomers, which can be formulated in a much wider range of conditions without altering the homogeneity of the obtained materials.

Besides the physical performance, the integration of lignin in PU materials could contribute to improve their environmental performance. In this respect, the Sels group has recently reported that reductive catalytic fractionation (another type of lignocellulose biorefining belonging to the family of "lignin-first" processes, similarly to the AAF process) generates an oligomeric fraction with a calculated global warming potential (GWP) of −0.949 kg CO_2.[68] This negative value indicates a net consumption of CO_2, that is, a net carbon capturing effect for the oligomer production. Although such a calculation was not reported yet for the AAF process, this negative value will most likely also apply for the AAF oligomers. Hence, the integration of AAF oligomers in PU materials will not only bring technical benefits but also contribute to decrease the GWP of the polymer industry.[2]

CONCLUSIONS

In order to unlock the full potential of lignocellulosic biomass, we need to study how all the fractions generated by a specific biorefining process could be individually valorized into added-value products. In this respect, the AAF protecting strategy appears as a very efficient process for converting native lignin into two highly valuable fractions, namely, the high-yield monomeric fraction that could be used, notably as high value

https://dx.doi.org/10.1021/acs.biomac.0c00927
Biomacromolecules 2020, 21, 4135−4148

fine-chemicals, and also the unique oligomeric fractions that could enable the design of a new biopolymer, as demonstrated in this work. This is in strong contrast with the Kraft process that was optimized for cellulose pulp production and that inevitably generates lignin byproducts/waste.

These AAF oligomers not only outperformed unfractionated technical lignin for the design of versatile PU materials but also demonstrated unique advantages compared to refined Kraft lignin fractions both in terms of structural composition (absence of sulfur, preservation of the more native linkages of lignin) and properties (enhanced miscibility in a wider range of solvents, lighter colors). Besides, our findings also demonstrate that the botanical origin of the wood (hardwood vs softwood) largely influence the structure of the oligomers and can thus also be used as a design tool for tuning the network properties.

The design of polyurethane materials from AAF lignin oligomers could bring some unique advantages to the polymer industry but could also pose some specific challenges that will need to be further addressed. Some of these advantages are the possibility to tune the PU network structure and properties based on lignin fractions (rather than on unpractical technical lignin or hypothetical lignin model compounds) and to lower the carbon footprint of PU materials. From the challenges side, the fact that AAF lignin oligomers are a mixture of compounds (with average molecular weight and average functionality) could appear problematic for the polymer industry which is still accustomed to rely almost exclusively on pure compounds as starting materials. The reproducibility of the process and the influences of both botanical (plant source) and environmental (e.g., season) factors on the composition of the oligomers also need to be evaluated in order to ensure the constant quality of the obtained fractions.

Traditional tools of polymer science were successfully combined with advanced lignocellulose biorefining to create semi-bioaromatic materials in which the structural variability and the fascinating richness of lignin chemistry led to the design of new materials with superior performances, both in technical and sustainable terms.

■ ASSOCIATED CONTENT

Supporting Information

The Supporting Information is available free of charge at https://pubs.acs.org/doi/10.1021/acs.biomac.0c00927.

Protocol for the aldehyde-assisted fractionation and hydrogenolysis of AH and AS oligomers, protocol for the pre-extraction of hardwood and softwood Kraft lignin, protocols for ^{31}P NMR and 2D NMR, additional details for the measurement protocols and characterizations, and additional figures (PDF)

■ AUTHOR INFORMATION

Corresponding Author

Richard Vendamme − *Flemish Institute for Technological Research (Vito N.V.), 2400 Mol, Belgium; Department of Materials and Chemistry, Physical Chemistry and Polymer Science, Vrije Universiteit Brussel, B-1050 Brussels, Belgium;* orcid.org/0000-0002-8931-0851; Email: richard.vendamme@vito.be

Authors

Jean Behaghel de Bueren − *Laboratory of Sustainable and Catalytic Processing, Institute of Chemical Sciences and Engineering, Ecole Polytechnique Fédérale de Lausanne, EPFL, 1015 Lausanne, Switzerland*

Jaime Gracia-Vitoria − *Flemish Institute for Technological Research (Vito N.V.), 2400 Mol, Belgium*

Florence Isnard − *Flemish Institute for Technological Research (Vito N.V.), 2400 Mol, Belgium*

Mikael Monga Mulunda − *Flemish Institute for Technological Research (Vito N.V.), 2400 Mol, Belgium; Department of Chemistry, University of Lubumbashi, 1825 Lubumbashi, D. R. Congo*

Pablo Ortiz − *Flemish Institute for Technological Research (Vito N.V.), 2400 Mol, Belgium;* orcid.org/0000-0002-3954-5409

Mohan Wadekar − *Flemish Institute for Technological Research (Vito N.V.), 2400 Mol, Belgium*

Karolien Vanbroekhoven − *Flemish Institute for Technological Research (Vito N.V.), 2400 Mol, Belgium*

Chloé Wegmann − *Laboratory of Sustainable and Catalytic Processing, Institute of Chemical Sciences and Engineering, Ecole Polytechnique Fédérale de Lausanne, EPFL, 1015 Lausanne, Switzerland*

Raymond Buser − *Laboratory of Sustainable and Catalytic Processing, Institute of Chemical Sciences and Engineering, Ecole Polytechnique Fédérale de Lausanne, EPFL, 1015 Lausanne, Switzerland*

Florent Héroguel − *Laboratory of Sustainable and Catalytic Processing, Institute of Chemical Sciences and Engineering, Ecole Polytechnique Fédérale de Lausanne, EPFL, 1015 Lausanne, Switzerland;* orcid.org/0000-0003-2210-7119

Jeremy S. Luterbacher − *Laboratory of Sustainable and Catalytic Processing, Institute of Chemical Sciences and Engineering, Ecole Polytechnique Fédérale de Lausanne, EPFL, 1015 Lausanne, Switzerland;* orcid.org/0000-0002-0967-0583

Walter Eevers − *Flemish Institute for Technological Research (Vito N.V.), 2400 Mol, Belgium; Department of Chemistry, University of Antwerp, 2020 Antwerp, Belgium*

Complete contact information is available at: https://pubs.acs.org/10.1021/acs.biomac.0c00927

Notes

The authors declare no competing financial interest.

■ ACKNOWLEDGMENTS

The authors from VITO are grateful to the province of Noord-Brabant (The Netherlands) for partially supporting this work in the framework of the activities at the Shared Research Center Biorizon.

■ REFERENCES

(1) Zimmerman, J. B.; Anastas, P. T.; Erythropel, H. C.; Leitner, W. Designing for a Green Chemistry Future. *Science* **2020**, *367*, 397−400.

(2) Zheng, J.; Suh, S. Strategies to Reduce the Global Carbon Footprint of Plastics. *Nat. Clim. Change* **2019**, *9*, 374−378.

(3) World Economic Forum (WEF). Top 10 Emerging Technologies 2019. *World Economic Forum Annual Meeting 2019*, 2019, No. June, 4−15.

(4) Feghali, E.; Torr, K. M.; van de Pas, D. J.; Ortiz, P.; Vanbroekhoven, K.; Eevers, W.; Vendamme, R. Thermosetting

Polymers from Lignin Model Compounds and Depolymerized Lignins. *Top. Curr. Chem.* **2018**, *376*, 32.
(5) Lora, J. H.; Glasser, W. G. Recent Industrial Applications of Lignin: A Sustainable Alternative to Nonrenewable Materials. *J. Polym. Environ.* **2002**, *10*, 39−48.
(6) Glasser, W. G. About Making Lignin Great Again—Some Lessons From the Past. *Front. Chem.* **2019**, *7*, 565.
(7) Pei, W.; Shang, W.; Liang, C.; Jiang, X.; Huang, C.; Yong, Q. Using Lignin as the Precursor to Synthesize Fe3O4@lignin Composite for Preparing Electromagnetic Wave Absorbing Lignin-Phenol-Formaldehyde Adhesive. *Ind. Crops Prod.* **2020**, *154*, 112638.
(8) Huang, C.; He, J.; Narron, R.; Wang, Y.; Yong, Q. Characterization of Kraft Lignin Fractions Obtained by Sequential Ultrafiltration and Their Potential Application as a Biobased Component in Blends with Polyethylene. *ACS Sustainable Chem. Eng.* **2017**, *5*, 11770−11779.
(9) Sonnenschein, M. F. *Polyurethanes*; John Wiley & Sons, Inc: Hoboken, NJ, 2014.
(10) Vendamme, R.; Schüwer, N.; Eevers, W. Recent Synthetic Approaches and Emerging Bio-Inspired Strategies for the Development of Sustainable Pressure-Sensitive Adhesives Derived from Renewable Building Blocks. *J. Appl. Polym. Sci.* **2014**, *131*, 8379−8394.
(11) Zhu, Y.; Romain, C.; Williams, C. K. Sustainable Polymers from Renewable Resources. *Nature* **2016**, *540*, 354−362.
(12) Rodrigues, A. E.; Pinto, P. C. d. O. R.; Barreiro, M. F.; Esteves da Costa, C. A.; Ferreira da Mota, M. I.; Fernandes, I. Polyurethanes from Recovered and Depolymerized Lignins. *An Integrated Approach for Added-Value Products from Lignocellulosic Biorefineries*; Springer International Publishing: Cham, 2018; pp 85−117.
(13) Alinejad, M.; Henry, C.; Nikafshar, S.; Gondaliya, A.; Bagheri, S.; Chen, N.; Singh, S.; Hodge, D.; Nejad, M. Lignin-Based Polyurethanes: Opportunities for Bio-Based Foams, Elastomers, Coatings and Adhesives. *Polymers* **2019**, *11*, 1202.
(14) Laurichesse, S.; Avérous, L. Chemical Modification of Lignins: Towards Biobased Polymers. *Prog. Polym. Sci.* **2014**, *39*, 1266−1290.
(15) Laurichesse, S.; Huillet, C.; Avérous, L. Original Polyols Based on Organosolv Lignin and Fatty Acids: New Bio-Based Building Blocks for Segmented Polyurethane Synthesis. *Green Chem.* **2014**, *16*, 3958−3970.
(16) Sadeghifar, H.; Cui, C.; Argyropoulos, D. S. Toward Thermoplastic Lignin Polymers. Part 1. Selective Masking of Phenolic Hydroxyl Groups in Kraft Lignins via Methylation and Oxypropylation Chemistries. *Ind. Eng. Chem. Res.* **2012**, *51*, 16713−16720.
(17) Dubreuil, M. F. S.; Servaes, K.; Ormerod, D.; Van Houtven, D.; Porto-Carrero, W.; Vandezande, P.; Vanermen, G.; Buekenhoudt, A. Selective Membrane Separation Technology for Biomass Valorization towards Bio-Aromatics. *Sep. Purif. Technol.* **2017**, *178*, 56−65.
(18) Passoni, V.; Scarica, C.; Levi, M.; Turri, S.; Griffini, G. Fractionation of Industrial Softwood Kraft Lignin: Solvent Selection as a Tool for Tailored Material Properties. *ACS Sustainable Chem. Eng.* **2016**, *4*, 2232−2242.
(19) Jiang, X.; Savithri, D.; Du, X.; Pawar, S.; Jameel, H.; Chang, H.-m.; Zhou, X. Fractionation and Characterization of Kraft Lignin by Sequential Precipitation with Various Organic Solvents. *ACS Sustain. Chem. Eng.* **2017**, *5*, 835−842.
(20) Wang, Y.-Y.; Li, M.; Wyman, C. E.; Cai, C. M.; Ragauskas, A. J. Fast Fractionation of Technical Lignins by Organic Cosolvents. *ACS Sustainable Chem. Eng.* **2018**, *6*, 6064−6072.
(21) Sadeghifar, H.; Ragauskas, A. Perspective on Technical Lignin Fractionation. *ACS Sustainable Chem. Eng.* **2020**, *8*, 8086.
(22) Gioia, C.; Lo Re, G.; Lawoko, M.; Berglund, L. Tunable Thermosetting Epoxies Based on Fractionated and Well-Characterized Lignins. *J. Am. Chem. Soc.* **2018**, *140*, 4054−4061.
(23) Griffini, G.; Passoni, V.; Suriano, R.; Levi, M.; Turri, S. Polyurethane Coatings Based on Chemically Unmodified Fractionated Lignin. *ACS Sustainable Chem. Eng.* **2015**, *3*, 1145−1154.
(24) Wang, Y.-Y.; Wyman, C. E.; Cai, C. M.; Ragauskas, A. J. Lignin-Based Polyurethanes from Unmodified Kraft Lignin Fractionated by Sequential Precipitation. *ACS Appl. Polym. Mater.* **2019**, *1*, 1672−1679.
(25) Cui, M.; Nguyen, N. A.; Bonnesen, P. V.; Uhrig, D.; Keum, J. K.; Naskar, A. K. Rigid Oligomer from Lignin in Designing of Tough, Self-Healing Elastomers. *ACS Macro Lett.* **2018**, *7*, 1328−1332.
(26) Schutyser, W.; Renders, T.; Van den Bosch, S.; Koelewijn, S.-F.; Beckham, G. T.; Sels, B. F. Chemicals from Lignin: An Interplay of Lignocellulose Fractionation, Depolymerisation, and Upgrading. *Chem. Soc. Rev.* **2018**, *47*, 852−908.
(27) Sun, Z.; Fridrich, B.; de Santi, A.; Elangovan, S.; Barta, K. Bright Side of Lignin Depolymerization: Toward New Platform Chemicals. *Chem. Rev.* **2018**, *118*, 614−678.
(28) Shuai, L.; Talebi Amiri, M.; Luterbacher, J. S. The influence of interunit carbon-carbon linkages during lignin upgrading. *Curr. Opin. Green Sustain. Chem.* **2016**, *2*, 59−63.
(29) Shuai, L.; Amiri, M. T.; Questell-Santiago, Y. M.; Héroguel, F.; Li, Y.; Kim, H.; Meilan, R.; Chapple, C.; Ralph, J.; Luterbacher, J. S. Formaldehyde Stabilization Facilitates Lignin Monomer Production during Biomass Depolymerization. *Science* **2016**, *354*, 329−333.
(30) Lan, W.; Amiri, M. T.; Hunston, C. M.; Luterbacher, J. S. Protection Group Effects During α,γ-Diol Lignin Stabilization Promote High-Selectivity Monomer Production. *Angew. Chem., Int. Ed.* **2018**, *130*, 1370−1374.
(31) Talebi Amiri, M.; Dick, G. R.; Questell-Santiago, Y. M.; Luterbacher, J. S. Fractionation of Lignocellulosic Biomass to Produce Uncondensed Aldehyde-Stabilized Lignin. *Nat. Protoc.* **2019**, *14*, 921−954.
(32) Questell-Santiago, Y. M.; Galkin, M. V.; Barta, K.; Luterbacher, J. S. Stabilization Strategies in Biomass Depolymerization Using Chemical Functionalization. *Nat. Rev. Chem.* **2020**, *4*, 311.
(33) Questell-Santiago, Y. M.; Zambrano-Varela, R.; Talebi Amiri, M.; Luterbacher, J. S. Carbohydrate Stabilization Extends the Kinetic Limits of Chemical Polysaccharide Depolymerization. *Nat. Chem.* **2018**, *10*, 1222−1228.
(34) van de Pas, D. J.; Torr, K. M. Biobased Epoxy Resins from Deconstructed Native Softwood Lignin. *Biomacromolecules* **2017**, *18*, 2640−2648.
(35) Kaiho, A.; Mazzarella, D.; Satake, M.; Kogo, M.; Sakai, R.; Watanabe, T. Construction of the di(trimethylolpropane) cross linkage and the phenylnaphthalene structure coupled with selective β-O-4 bond cleavage for synthesizing lignin-based epoxy resins with a controlled glass transition temperature. *Green Chem.* **2016**, *18*, 6526−6535.
(36) Meng, X.; Crestini, C.; Ben, H.; Hao, N.; Pu, Y.; Ragauskas, A. J.; Argyropoulos, D. S. Determination of Hydroxyl Groups in Biorefinery Resources via Quantitative 31P NMR Spectroscopy. *Nat. Protoc.* **2019**, *14*, 2627−2647.
(37) Hu, Z.; Du, X.; Liu, J.; Chang, H.-m.; Jameel, H. Structural Characterization of Pine Kraft Lignin: BioChoice Lignin vs Indulin AT. *J. Wood Chem. Technol.* **2016**, *36*, 432−446.
(38) Constant, S.; Wienk, H. L. J.; Frissen, A. E.; Peinder, P. d.; Boelens, R.; Van Es, D. S.; Grisel, R. J. H.; Weckhuysen, B. M.; Huijgen, W. J. J.; Gosselink, R. J. A.; Bruijnincx, P. C. A. New Insights into the Structure and Composition of Technical Lignins: A Comparative Characterisation Study. *Green Chem.* **2016**, *18*, 2651−2665.
(39) Heitner, C.; Dimmel, D. R.; Schmidt, J. A. *Lignin and Lignans Advances in Chemistry*; CRC Press, 2010.
(40) Zijlstra, D. S.; de Santi, A.; Oldenburger, B.; de Vries, J.; Barta, K.; Deuss, P. J. Extraction of Lignin with High β-O-4 Content by Mild Ethanol Extraction and Its Effect on the Depolymerization Yield. *J. Vis. Exp.* **2019**, *143*, No. e58575.
(41) Ralph, J.; Lapierre, C.; Boerjan, W. Lignin Structure and Its Engineering. *Curr. Opin. Biotechnol.* **2019**, *56*, 240−249.
(42) Thielemans, W.; Wool, R. P. Lignin Esters for Use in Unsaturated Thermosets: Lignin Modification and Solubility Modeling. *Biomacromolecules* **2005**, *6*, 1895−1905.

https://dx.doi.org/10.1021/acs.biomac.0c00927
Biomacromolecules 2020, 21, 4135−4148

(43) Sameni, J.; Krigstin, S.; Sain, M. Solubility of Lignin and Acetylated Lignin in Organic Solvents. *BioResources* **2017**, *12*, 1548−1565.
(44) Wadekar, M.; Eevers, W.; Vendamme, R. Influencing the Properties of LigninPU Films by Changing Copolyol Chain Length, Lignin Content and NCO/OH Mol Ratio. *Ind. Crops Prod.* **2019**, *141*, 111665.
(45) De Haro, J. C.; Allegretti, C.; Smit, A. T.; Turri, S.; D'Arrigo, P.; Griffini, G. Biobased Polyurethane Coatings with High Biomass Content: Tailored Properties by Lignin Selection. *ACS Sustainable Chem. Eng.* **2019**, *7*, 11700−11711.
(46) Klein, S. E.; Rumpf, J.; Kusch, P.; Albach, R.; Rehahn, M.; Witzleben, S.; Schulze, M. Unmodified Kraft Lignin Isolated at Room Temperature from Aqueous Solution for Preparation of Highly Flexible Transparent Polyurethane Coatings. *RSC Adv.* **2018**, *8*, 40765−40777.
(47) Ciobanu, C.; Ungureanu, M.; Ignat, L.; Ungureanu, D.; Popa, V. I. Properties of Lignin-Polyurethane Films Prepared by Casting Method. *Ind. Crops Prod.* **2004**, *20*, 231−241.
(48) Halley, P. J.; Graeme, G. A. *Chemorheology of Polymers: From Fundamental Principles to Reactive Processing*; Cambridge University Press, 2009.
(49) Erman, B.; Mark, J. E. *Structures and Properties of Rubberlike Networks*; Oxford University Press: New York, 1997.
(50) Flory, P. J. *Principles of Polymer Chemistry*; Cornell University Press, 1953.
(51) De Gennes, P. G. *Scaling Concepts in Polymer Physics*; Cornell University Press, 1979.
(52) Urayama, K.; Miki, T.; Takigawa, T.; Kohjiya, S. Damping Elastomer Based on Model Irregular Networks of End-Linked Poly(Dimethylsiloxane). *Chem. Mater.* **2004**, *16*, 173−178.
(53) Vainio, U.; Maximova, N.; Hortling, B.; Laine, J.; Stenius, P.; Simola, L. K.; Gravitis, J.; Serimaa, R. Morphology of Dry Lignins and Size and Shape of Dissolved Kraft Lignin Particles by X-Ray Scattering. *Langmuir* **2004**, *20*, 9736−9744.
(54) Goudarzi, A.; Lin, L.-T.; Ko, F. K. X-Ray Diffraction Analysis of Kraft Lignins and Lignin-Derived Carbon Nanofibers. *J. Nanotechnol. Eng. Med.* **2014**, *5*, 021006.
(55) Trovati, G.; Sanches, E. A.; Neto, S. C.; Mascarenhas, Y. P.; Chierice, G. O. Characterization of Polyurethane Resins by FTIR, TGA, and XRD. *J. Appl. Polym. Sci.* **2010**, *115*, 263−268.
(56) Li, Y.; Sarkanen, S. Miscible Blends of Kraft Lignin Derivatives with Low-TgPolymers. *Macromolecules* **2005**, *38*, 2296−2306.
(57) Wang, Y.-Y.; Chen, Y.-r.; Sarkanen, S. Path to Plastics Composed of Ligninsulphonates (Lignosulfonates). *Green Chem.* **2015**, *17*, 5069−5078.
(58) Gioia, C.; Colonna, M.; Tagami, A.; Medina, L.; Sevastyanova, O.; Berglund, L. A.; Lawoko, M. Lignin-Based Epoxy Resins: Unravelling the Relationship between Structure and Material Properties. *Biomacromolecules* **2020**, *21*, 1920−1928.
(59) Gent, A. N. A New Constitutive Relation for Rubber. *Rubber Chem. Technol.* **1996**, *69*, 59−61.
(60) Tran, C. D.; Chen, J.; Keum, J. K.; Naskar, A. K. A New Class of Renewable Thermoplastics with Extraordinary Performance from Nanostructured Lignin-Elastomers. *Adv. Funct. Mater.* **2016**, *26*, 2677−2685.
(61) Vendamme, R.; Eevers, W. Sticky Degradable Bioelastomers. *Chem. Mater.* **2017**, *29*, 5353−5363.
(62) Creton, C.; Ciccotti, M. Fracture and Adhesion of Soft Materials: A Review. *Rep. Prog. Phys.* **2016**, *79*, 046601.
(63) Mark, J. E.; Andrady, A. L. Model Networks of End-Linked Polydimethylsiloxane Chains. X. Bimodal Networks Prepared in Two-Stage Reactions Designed to Give High Spatial Heterogeneity. *Rubber Chem. Technol.* **1981**, *54*, 366−373.
(64) Tavares, L. B.; Boas, C. V.; Schleder, G. R.; Nacas, A. M.; Rosa, D. S.; Santos, D. J. Bio-Based Polyurethane Prepared from Kraft Lignin and Modified Castor Oil. *Express Polym. Lett.* **2016**, *10*, 927−940.
(65) Li, H.; Sun, J.-T.; Wang, C.; Liu, S.; Yuan, D.; Zhou, X.; Tan, J.; Stubbs, L.; He, C. High Modulus, Strength, and Toughness Polyurethane Elastomer Based on Unmodified Lignin. *ACS Sustainable Chem. Eng.* **2017**, *5*, 7942−7949.
(66) Naskar, A. K.; Keum, J. K.; Boeman, R. G. Polymer Matrix Nanocomposites for Automotive Structural Components. *Nat. Nanotechnol.* **2016**, *11*, 1026−1030.
(67) Liff, S. M.; Kumar, N.; McKinley, G. H. High-Performance Elastomeric Nanocomposites via Solvent-Exchange Processing. *Nat. Mater.* **2007**, *6*, 76−83.
(68) Liao, Y.; Koelewijn, S.-F.; van den Bossche, G.; van Aelst, J.; van den Bosch, S.; Renders, T.; Navare, K.; Nicolaï, T.; van Aelst, K.; Maesen, M.; Matsushima, H.; Thevelein, J. M.; van Acker, K.; Lagrain, B.; Verboekend, D.; Sels, B. F. A Sustainable Wood Biorefinery for Low-Carbon Footprint Chemicals Production. *Science* **2020**, *367*, 1385−1390.

https://dx.doi.org/10.1021/acs.biomac.0c00927
Biomacromolecules 2020, 21, 4135−4148